

# RSC Advances



This is an *Accepted Manuscript*, which has been through the Royal Society of Chemistry peer review process and has been accepted for publication.

*Accepted Manuscripts* are published online shortly after acceptance, before technical editing, formatting and proof reading. Using this free service, authors can make their results available to the community, in citable form, before we publish the edited article. This *Accepted Manuscript* will be replaced by the edited, formatted and paginated article as soon as this is available.

You can find more information about *Accepted Manuscripts* in the [Information for Authors](#).

Please note that technical editing may introduce minor changes to the text and/or graphics, which may alter content. The journal's standard [Terms & Conditions](#) and the [Ethical guidelines](#) still apply. In no event shall the Royal Society of Chemistry be held responsible for any errors or omissions in this *Accepted Manuscript* or any consequences arising from the use of any information it contains.

1 **Modeling of gas generation from the river adjacent to the**  
2 **manufactured gas plant**

3

4 **Tengyi Zhu<sup>1,2</sup>, Dafang Fu<sup>1\*</sup>, Chad T. Jafvert<sup>2</sup>, Rajendra Prasad Singh<sup>1,2</sup>**

5 *<sup>1</sup>School of Civil Engineering, Southeast University, Nanjing, 210096, China*

6 *<sup>2</sup>School of Civil Engineering, Purdue University, West Lafayette, IN 47907, USA*

7

8

9

10

11

12

13

14

15

16

17

18

19

20

21

22

23

24 \*Corresponding author, Tel: 086+18761882638

25 E-mail address: fdf@seu.edu.cn (Dafang Fu)

26 **Abstract**

27 Ebullition of gas bubbles through sediment can enhance the migration of gases through the  
28 subsurface and potentially effect the emission of important greenhouse gases to the atmosphere. To  
29 better understand the parameters controlling ebullition, investigations of the gas ebullition in Grand  
30 Calumet river (Indiana, USA) were conducted. We found that gas ebullition might shift and change  
31 in different vertical hydraulic gradient and temperature. The CO<sub>2</sub> and CH<sub>4</sub> flux for each site increased  
32 with increase of temperature. A comparatively simple linear relationship existed between gas flux and  
33 measured parameters ( $G_F = 0.316 T + 300.66i$ ,  $R^2 = 0.82$ ). The gas flux in sand cap was more variable  
34 than that in sediment. Besides, the total field gas fluxes varied from 10 to 180 mmole m<sup>-2</sup> d<sup>-1</sup> for  
35 sediment and from 5 to 35 mmole m<sup>-2</sup> d<sup>-1</sup> for sand cap, which proved in situ sand cap could be an  
36 effective remediation. The analysis presented here has shown that gas flues and reactive transport  
37 modeling can provide effective means of investigating ebullition and quantifying gas transport.

38

39

40

41

42

43

44

45

46

47

48 **Keywords:** Gas ebullition, Sand cap, Pore water flux, Tar migration

49

## 50 1. Introduction

51 Freshwater resources pollution by various organic and inorganic contaminants such as Polycyclic  
52 Aromatic Hydrocarbons (PAHs) and other chemicals becomes a concern to the researchers. Studies  
53 were conducted to investigate the gas ebullition, PAHs contaminants and to better characterize the  
54 existing hydrologic conditions around and within a river adjacent to a former manufactured gas plant  
55 (MGP) site at Grand Calumet river, Indiana, USA.<sup>1,2</sup> Surface water of Grand Calumet river indicated  
56 that tar and oil droplets migration from sediment was occurring near the former gas station. These  
57 indications were problematic, because the tar was a dense non aqueous phase liquid (DNAPL), once  
58 it was deposited in riverbed sediment, one typically would not expect it to float up from the riverbed  
59 to the water surface.

60 Different aspects of facilitated migration of contaminants from sediments have been investigated by  
61 many researchers, in particular the gas generation from sediment. Gas migration from sediment was  
62 found to be a function of changes in air pressure.<sup>3</sup> Changes in hydrostatic pressure due to changing  
63 elevation also were found at several field sites to influence rates of gas migration.<sup>4</sup> Sediment  
64 temperature was found to influence gas migration from sediment in Lake Sawa, Japan, on a seasonal  
65 basis.<sup>5</sup> Long-term trends for methane mass in water were evaluated at Onondaga Lake in New York,  
66 USA, and it was found that methane increased through the spring and summer, peaked in early fall,  
67 and rapidly decreased in late fall to winter.<sup>6,7</sup>

68 Although ebullition was accepted as a potentially important mechanism for the fate of contaminants,  
69 no comprehensive studies have reported in literature related to the temperature and elevation effect on  
70 it. Palermo *et al.*<sup>8</sup> found that gas ebullition can have a significant effect on sediment stability.  
71 Ebullition was the result of a series of processes in which excess gases were generated by  
72 micro-organisms from organic matter. The gases release from contaminated sediments were generally  
73 methane (46-95%), nitrogen (3-50%), and trace amounts of hydrogen, carbon dioxide, ammonia, and  
74 hydrogen sulfide.<sup>9</sup> Most of the gas bubbles originate from the upper 10-20 cm of the sediment  
75 column.<sup>10</sup> Martens and Klump<sup>11</sup> reported a range of bubble sizes between 0.062 cm and 0.37 cm with  
76 a mean volume of 0.104 ml at a water depth of 7.5 m. Bubbles grew until a pressure threshold was  
77 reached as they had to build up a certain amount of buoyancy to overcome the cohesive strength of the  
78 sediment and migrate upward. Gas ebullition generally occurred episodically due to changes in  
79 pressure and water level which influenced the sediment matrix and thus affected the gas bubble  
80 release.<sup>10</sup> Increased hydraulic gradients, atmospheric pressure changes led to a sudden release of gas  
81 bubbles which ceases after the excess pressure is relieved. Data revealed that size of the gas bubble  
82 depended on the amount of the gas in bubbles, temperature and pressure, where temperature strongly

83 affected microbial activities as well as the saturation of the gas.<sup>8</sup> Therefore, the purpose of this study  
84 was to investigate the rate of gas ebullition and tried to build a gas ebullition model using multivariate  
85 regression analysis. In addition, understanding the facilitated migration of the NAPL process is  
86 necessary to formulate remedies to reduce the risk from the tarry sediment.

## 87 **2. Materials and Methods**

### 88 *2.1 Gas collection and analysis*

89 The volume of gas released from the sediment was measured using “gas tents” at five locations  
90 within Reach 6, six locations within Reach 7, and one location within Reach 5. Additionally, gas was  
91 collected from four of the sand cap test cells, with seepage meter domes in Reach 6. The test cells were  
92 installed by Purdue in 2008, and the two sand-only caps and the two sand-organoclay caps were  
93 monitored. The sediment near each of these test cells was sampled at the same time as each of the sand  
94 caps for comparisons. Fig. 1 showed the general location of gas sampling activities.

95

[Fig. 1]

96 Each gas “tent” (Fig. 2) consisted of a frame made from PVC pipe (Schedule 40, 7.6 cm ID) and  
97 PVC film (0.2 mm thickness). The area of each gas tent was 6.5 m<sup>2</sup> (3.05 m by 2.13 m). Each tent was  
98 held in place with 4 PVC pipes pushed into the sediment. In this way, each gas tent could move  
99 vertically as the river elevation changed by floating on the surface of the river. A closable sampling  
100 port (vent) was installed through the film near one of the corners. Upon sampling, the input port of an  
101 electric pump was attached to the port of the tent, and the output end of the pump to 0.5, 8.1, or 20.3 L  
102 Tedlar gas sampling bag. Bags in series were filled completely by squeegeeing the gas (under the PVC  
103 film) to the corner where the gas at the vent was actively pumped. To sample the gas released from the  
104 sand cap test cells and the adjacent sediment in Reach 6, seepage meter domes were placed in the sand  
105 and adjacent sediment, respectively. The area covered by a seepage meter dome was 0.3 m<sup>2</sup>, and the  
106 port that normally would be connected to the seepage meter flow tube was capped such as all gas  
107 emitted from the sediment was collected in a gas sampling bag attached to the central pipe through a  
108 connector-valve and flexible tubing (Fig. 2). For each gas sampling event for both the gas tent  
109 experiments and the sand cap experiments, gas was collected for at least 7 days, removing (collecting)  
110 the gas every few days into the Tedlar bags to measure the volume. Gas ebullition was clearly evident,  
111 as streams of bubbles were often observed emanating from the river after a sufficient quiescent period.  
112 Alternatively, during the summer, gas release could be induced simply by disturbing the water or  
113 sediment surface with a boat oar.

114 Gases were collected into gas bags and then 1ml gas was subsampled into evacuated 12 ml labco  
115 exetainers (Labco Limited, UK). The analysis was carried by using a PDZ-Europa trace gas analyzer  
116 (TGA) interfaced to a 20/20 PDZ-Europa isotopic ratio mass spectrometer (IRMS) (Sercon, Crewe,  
117 UK).

118 [Fig. 2]

## 119 2.2 Seepage meter

120 The interfacial flow measuring system consisted of a dome with flow tube and vent, circuit board,  
121 and computer (Fig. 3). The dome made by stainless steel had an OD of 61 cm, the height of 19.1 cm,  
122 and volume capacity of 28.4 L. The gas vent was a 1.27 cm diameter PVC pipe attached to the top of  
123 the dome with a bulk-head flange was of sufficient length to extend above the water surface, allowing  
124 gas to escape and water to rise within the pipe to the river's water table level. Closed-cell polyurethane  
125 foam, attached to the rim of the dome ensures a water-tight seal. The flux meter and the dome were  
126 connected directly using a flow tube. This allowed water to flow between the river and the flux meter  
127 at a volumetric rate equal to the rate across the sediment-water surface. As water flowed through the  
128 tube, the four thermocouples positioned within the tube at different positions sense the temperature  
129 change as a function of time. The volumetric flow rate in the tube was calculated from the  
130 temperature-time profile measured by the two thermocouples downstream from the heater, as  
131 described in our previous study.<sup>1</sup>

132 [Fig. 3]

133 Sediment at the experimental site of Grand Calumet river was composed generally of silt sized  
134 particles with high organic matter, consisting of both natural organic matter and coal-tar as reported in  
135 our previous study.<sup>10</sup> Fine to medium grain sand layer occurred below this organic rich top layer.  
136 Interfacial flow (Darcy flux) was measured at 7 locations (3 within Reach 6 and 4 within Reach 7),  
137 (Table S1). Measurements were made at each location between 4 and 8 times over a 15 month period.  
138 The first measurement was made near RC3 on March 28, 2011, and the last measurement was made  
139 near RC12 on May 25, 2012. On each day at each location, generally between 2 and 6 measurements  
140 were made, each requiring approximately 30 to 40 minutes, with the reported Darcy velocity being the  
141 average of all values recorded.

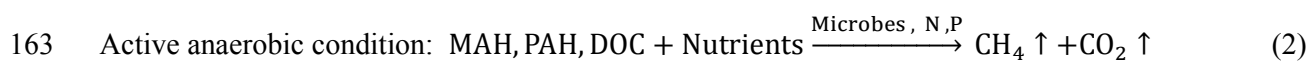
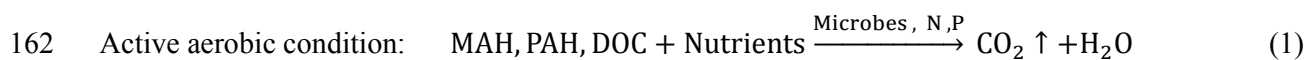
### 142 2.3 Installation of piezometer

143 There were fifty piezometers, gas collector sheets and eight stream gauges were installed to  
 144 monitor the local hydrology and gas ebullition along a 2.5 km stretch of Grand Calumet river (Fig.  
 145 1). Piezometers were constructed from 4.45 cm OD polyethylene pipe with 20 holes (0.95 cm diameter)  
 146 drilled into the pipe within 15.2 cm of the capped end. These holes were wrapped with a porous  
 147 geotextile and aluminum wire mesh to avoid sediment inflow and clogging. The stream gauges (i.e.,  
 148 piezometer at depth 0) were constructed in the same manner with the holes and screen located within a  
 149 60 cm segment at a sufficient distance from the capped end to assure they would be located above the  
 150 sediment-water interface after installation. The piezometers and stream gauges were installed  
 151 manually by pushing to the target depth. In the river, six piezometer clusters were installed, with each  
 152 cluster consisting of two piezometers pushed to depths of 1.2 and 2.4 m below the sediment–water  
 153 interface, and one stream gauge, each located approximately 15 cm apart. The location of each cluster  
 154 is shown on Fig. 1 and Fig. 3.

## 155 3. Results and Discussions

### 156 3.1 Effect of gas ebullition

157 As shown in Fig. 4, below the water surface 2.0-3.3 m organic-rich sediment layer was 0.3-0.6 m of  
 158 a fine to medium grain sand layer over a continuous less permeable clay layer. The sand layer was  
 159 extensive enough to be connected, but not evenly distributed over the site. It presented the schematic  
 160 of the basic hydro-biogeochemical processes occurring within the sediment as it currently existed (Eq.  
 161 1 and 2).



164 [Fig. 4, 5]

165 The measured total field gas fluxes varied from 10 to 180  $\text{mmole m}^{-2} \text{d}^{-1}$  for sediment and from 5 to  
 166 35  $\text{mmole m}^{-2} \text{d}^{-1}$  for sand cap (Fig. 5). Overall,  $\text{CH}_4$ ,  $\text{N}_2$ , and  $\text{CO}_2$  comprised  $54.44 \pm 8.22 \%$ ,  $39.72 \pm$   
 167  $8.92 \%$ , and  $5.83 \pm 1.21 \%$  (values are means  $\pm$  SD) of the gas by volume, respectively. The gas  
 168 ebullition was higher at reach 6, reach 7 and sediment, whereas release of gas at reach 5 and sand cap

169 was comparatively lower. It was due to the low activity and PAHs at the sand cap layer on  
170 contaminated sediment as described by Mclinn and Stolzenburg.<sup>3</sup> It was clear from Figure 5b that the  
171 gas flux value of sediment dome was lower than that in sediment PVC device. The reasons were as  
172 follows: in comparison to sediment-water interface, there was gas flux in water-air interface which  
173 was decomposed by environment microbe in river water. In addition, the content of N<sub>2</sub> has high  
174 percentage in the air (78.12%), which solubility is 1/50 by volume. N<sub>2</sub> dissolved in the water could  
175 be collected with PVC device by flowing water. Analysis of simulated CH<sub>4</sub> transport provides a  
176 measure of the significance of ebullition as a transport mechanism. At RC7b, the total gas produced  
177 was 128 mmole m<sup>2</sup> d<sup>-1</sup>. These large episodic releases indicated that they are commonly not coincident  
178 with short-term changes in water table elevation. Therefore many ebullition fluxes may be largely  
179 transparent to chamber- and tower-based measurements, and to methods that rely on changing water  
180 table elevation to estimate methane fluxes.<sup>12, 13</sup>

181 **[Fig. 6]**

182 As shown in Figure 6, the CO<sub>2</sub> and CH<sub>4</sub> flux for each site increased with increase of temperature.  
183 Higher temperatures in spring and summer led to higher  $G_F$  compared to fall. The relationship  
184 between CH<sub>4</sub> flux of sediment and water temperature was consistent with the results of Delsontro *et*  
185 *al.*<sup>12</sup>. And it was clear that the CO<sub>2</sub> and CH<sub>4</sub> flux values of sediment were higher than that in sand  
186 cap. Compare Fig. 6c with Fig. 6f, gas flux in sand cap was more variable than that in sediment. The  
187 reason maybe the complex system in sand cap. No bioturbation exists at the cap-sediment interface,  
188 and chemical migration processes are also much slower. Therefore, the upward migration of  
189 contaminants goes through the sand cap in sediment. The cap materials prevent pollutants enter into  
190 the water by adsorption, entrapment, bondage and degradation.<sup>14-16</sup> This function is very similar to  
191 the active cap layer or active permeable wall in the treatment of groundwater contamination.<sup>14</sup>  
192 Compared to the sediment, the permeability of the sand cap is better, but the volume of the gas flux  
193 is lower, which could be due to the sand cap aerobic microbial activity is higher, however, the  
194 anaerobic conditions exist in sediment, therefore the volume of gas fluxes in sediment was  
195 significantly higher than that in the sand cap (Fig. 5).

196 *3.2 Effect of Hydraulic Head, Darcy flux,*



197 The piezometric head  $h$ , is a measurement of the hydraulic head at the point of measurement  
 198 referenced to some standard elevation. From  $h$  values measured in the river stage ( $h_0$ ), 1.2 m deep  
 199 ( $h_{1.2}$ ), and 2.4 m deep ( $h_{2.4}$ ), piezometers at each piezometer cluster, vertical hydraulic head gradients  
 200  $i$  ( $\text{m m}^{-1}$ ), were calculated by dividing the hydraulic head differences between the piezometers by the  
 201 depth difference  $dz$ ,

$$202 \quad i_{a-b} = \frac{h_b - h_a}{dz} \quad (3)$$

203 Where, the subscripts  $a$  and  $b$  refer to the position within the sediment where the head was measured  
 204 relative to the sediment-water interface ( $h_a$  is always river level;  $h_b$  is the head in one of the  
 205 piezometers,  $dz = 1.2$  m). As shown on Figure 7, the water levels within the 1.2 piezometers were  
 206 generally higher than the river elevation, over the 5 months of continuous measurement from early  
 207 May to early September, 2012. The temporal changes in the gradients were minimal, except after  
 208 high rainfall events when the changes in elevation of the river ( $h_0$ ) was significant than the changes  
 209 in water levels within the 1.2 piezometers ( $p > 0.05$ ) (e.g., see May 8th, June 17th and August 26).

210 The vertical Darcy velocities or specific discharges,  $q$ , measured at each river cluster position are  
 211 reported in Table S1. The vertical hydraulic head gradients ( $i$ ) at each respective river cluster measured  
 212 manually on the same day when  $q$  was measured. Over all measurements, the range in the specific  
 213 discharge ( $q$ ) was  $0.24 - 2.53 \text{ cm d}^{-1}$ .

214 Note that reported the values of the vertical change in hydraulic head (i.e.; magnitude in positive or  
 215 negative head) was reflected in the corresponding seepage rates that were measured according to  
 216 Darcy's Law. The vertical hydraulic conductivity,  $K_v$  ( $\text{cm d}^{-1}$ ), within the top 1.2 m sediment layer is  
 217 calculated by dividing  $q$  by the corresponding hydraulic head gradient,  $i_{0-1.2}$ ,

$$218 \quad K_v = q \times i_{0-1.2}^{-1} = q \times \left(\frac{dh}{dz}\right)^{-1} \quad (4)$$

219 Where,  $dh$  is the piezometric head difference between the stream gauge and the 1.2-m piezometer,  
 220 and  $dz$  is the elevation difference between the sediment-water interface and 1.2-m piezometer screen  
 221 (i.e., 1.2m). The calculated values of  $K_v$  are reported in Table S1 with values ranging from  $1.26 \times 10^{-5}$   
 222 to  $2.93 \times 10^{-3} \text{ cm s}^{-1}$ . The major advantage of the interfacial flow meter system described in this study  
 223 is the ease with which it can be deployed to measure relatively low flow rates across the  
 224 sediment-water boundary. Under the lowest flux condition (e.g.,  $q = 0.29 \text{ cm d}^{-1}$  for RC11 on

225 5/22/2012; Table S1) discharge across the sediment-water interface through the area circumscribed  
226 by the collar was  $0.49 \text{ ml min}^{-1}$ . With an accurate addition of  $3.00 \text{ ml min}^{-1}$  with the pump, the  
227 fraction of flow due to groundwater discharge was nearly 30%, providing an accurate measurement  
228 even at this low flow rate. In some cases, measurements were made with the flow of water into the  
229 dome in alternate directions at the same arbitrary flow rate, such that the measured rate of discharge  
230 through the tube was either (a) actual flow + pump flow, or (b) actual flow - pump flow. In the latter  
231 case, the net flow direction was into the dome requiring  $T_m$  (the maximum temperature occurs at  
232 each thermocouple) to be measured at the thermocouple on the other side of the heater, nearest to the  
233 heater. In this case, the net ground water flow rate is simply the summation of two measured flow  
234 rates divided by 2, avoiding the need to accurately determine the pump flow rate.

235 Discharge and recharge of water from sediment had great influence on the release of gas from tar  
236 contaminated river beds. Figure 7 revealed the recharge and discharge trends on different study sites at  
237 different depth of river sediment. As shown in Fig. 7a, vertical gradient data at 1.2-2.4 m, RC6, RC5,  
238 RC7, RC8 and RC11 had higher vertical discharge, whereas recharge gradient values were found very  
239 low at these sites. The gas ebullition rate was also very high at sites where vertical gradient discharge  
240 was high. This trend indicated that release of gas also depended on the vertical gradient discharge. The  
241 possible reason for this trend might be the pressure release from the site resulted in higher release of  
242 gas. The discharge and recharge of vertical gradient rate at 0-1.2 m were not similar as that at 1.2-2.4 m.  
243 The deep sediments had high pressure that was responsible for release of gas. Increased hydraulic  
244 pressure and vertical gradient or hydrostatic pressure led to a higher release of gas bubbles which  
245 ceased after the excess pressure was relieved.

246 [Fig. 7]

247 In case of high pressure and discharge rate in sediments, the sediment layer could force newly  
248 generated gas bubbles to migrate through the available pores that resulted in breaking up larger  
249 bubbles into smaller ones. These bubbles then broke the sediment layer and flew upward according  
250 to the vertical gradient discharge trend and pressure into sediments. The size of the gas bubbles and  
251 their release rate depended on the amount of gas present in sediments, ambient temperature and  
252 pressure.

253 3.3 *Effect of Gas flux, Elevation, Tar migration*

254 [Fig. 8]

255 Water elevation played very important role in gas ebullition. It generated pressure in sediment that  
256 was responsible for forcing gas bubbles to transport upwards. Fig. 8 showed that gas flux was  
257 fluctuating according to the changes in river elevation. It revealed that the gas flux decreased as river  
258 level increased. The value of gas flux collected by plastic film for sediment was highest, and the value  
259 of test cell for sediment was higher than sand cap at the same time. High elevation generated pressure  
260 on sediment layer or sand cap, which forced gas bubbles to move upwards. It could be also concluded  
261 that sand cap were still very effective for reducing contaminant's upward flow. The impact of the gas  
262 flux and seepage depended on the rate of fluxes and therefore in-situ measurements of these fluxes  
263 were required.

264 Pore water flow through the sediments was presumably driven by piezometric head gradients that  
265 varied in time due to hydrologic processes. In estuaries, the effects may exhibit shorter time responses  
266 due to tidal fluctuations which can create short term variations in the head differences. The highest  
267 groundwater discharge corresponds with periods of low water level and could potentially even reverse  
268 direction. In the Grand Calumet river, reported measurements of seepage rates ranged from 0.24 to  
269 2.53 cm d<sup>-1</sup>. The groundwater seepage phenomenon could indirectly affect the stability of sediments  
270 by altering the consolidation rates in the sediment and changing the bulk density, and thus the erosion  
271 resistance. Simon and Collision<sup>12</sup> stated that in addition to the advective flow induced shear stresses  
272 on cohesive stream beds, another mechanism contributing to the detachment of cohesive aggregates is  
273 upward-directed seepage forces. The range of groundwater fluxes reported in the literature varied  
274 significantly, which depended on the sediment type of the bed and other characteristics of the site.  
275 Spatial and seasonal variations in the sites where seepage measurements were collected also affected  
276 the ranges. Since a vertical upwards gradient of greater than one implied a quick condition, the bed  
277 should not be stable due to seepage effects. One possible explanation was that non-Darcy flow through  
278 channels may be responsible for the primary transport of pore water through the sediments. This  
279 preferred flow would change many aspects of sediment resuspension and mass transfer of  
280 contaminants, which should be carefully considered for relevance at a particular site. Experimental

281 investigations studying seepage effect should be performed considering the possibility of channel  
282 formation.

### 283 3.4 Linear Regression Analysis Describes Gas Ebullition

284 A comparatively simple linear relationship existed between gas flux and measured parameters, as  
285 shown by multivariate regression analysis:

$$286 \quad G_F = 0.316 T + 300.66i, R^2 = 0.82 \quad (5)$$

287 Where  $G_F$  is molar gas flux ( $\text{mmole m}^{-2} \text{d}^{-1}$ ),  $T$  is pore water temperature ( $^{\circ}\text{C}$ ) and  $i$  represents the  
288 vertical hydraulic gradient ( $\text{m m}^{-1}$ ).

289 Under the recharge direction, there would be no relationship between gas flux and vertical  
290 hydraulic gradient. As shown in Fig. 7 and Fig. 8, all of vertical gradient data had higher vertical  
291 discharge and recharge gradient values were very low in our studies. It indicated that the release of  
292 gas also depended on the vertical gradient discharge. As shown in Fig. 9b, Methane flux increased as  
293 the vertical hydraulic gradient (discharge) went up. The results were consistent with the previous  
294 trend described by Huls and Costello.<sup>17</sup> In previous studies, if the discharge rate was high, gas  
295 ebullition was also high, which could affect the erosion rates.<sup>18</sup>

296 **[Fig. 9]**

297 Exploratory factor analysis was performed to assess the robustness of this regression. There were  
298 few studies reported in literature related to the temperature and gas flux. However, there were rare in  
299 the literature about the parameters of  $G_F$ , sediment temperature, and vertical hydraulic gradient.  
300 Moreover, no gas ebullition model was reported on the relationship between the vertical hydraulic  
301 gradient and the gas flux in the field. There were two models available in the literature corrected to  
302 gas fluxes<sup>19</sup>. The model results were converted from a volumetric basis assuming that the top 1 m of  
303 the sediment at the field sites is ebullition active to provide a consistent comparison to the measured  
304  $G_F$  values and the regression. Both literature models predict substantially higher  $G_F$  than those  
305 observed in the field. As shown in Fig. 9a, the calculated gas flux matched the measured values  
306 better ( $R^2 = 0.82$ ). Comparison of previous research, these two parameters were able to predict  $G_F$   
307 better than all the other measured parameters, explaining 82% of the variation (Fig. 9a). The choice  
308 of model for estimating volume of gas within the soil at the bog site depends on the elasticity of the

309 semipermeable, semiconfining layers that allow an interval of overpressured sediment to exist at  
310 depth. Rosenberry *et al.*<sup>13</sup> provided a gas ebullition model based on barometric efficiency, this model  
311 is not sensitive to the difference between porosity and volumetric moisture content of the sediment.  
312 Since the Grand Calumet river has a substantially overpressured interval at depth, it may be  
313 reasonable to prefer the overpressuring (or hydraulic head) model over the barometric efficiency  
314 model.<sup>13</sup> Beckwith and Baird<sup>20</sup> carried out a laboratory column study using time domain  
315 reflectometry probes that indicated a gas content between 5% and 10% by volume. These methods  
316 do not provide a direct, in situ measurement for gas volume. The methods described above are based  
317 on a destructive/invasive sampling methodology. Sediment samples were collected from peatlands,  
318 some of which had been dewatered by natural or man-made causes.<sup>13</sup> They were also instantaneous  
319 measurements. Methods used in this paper are noninvasive and nondestructive. In addition to  
320 providing an in-situ measure of gas volume, methods presented here provide continuous data,  
321 allowing the response of gas volume at different site to be related to climatic drivers. There is no  
322 paper reported that the difference between air-water interface and sediment-water interface gas  
323 collection.

324 Gas bubbles from sediment of the tar deposit were generated by anaerobic degradation of organic  
325 matter, consisting of organic material in the riverbed (sawdust and other detritus), as well as low  
326 molecular weight (LMW) PAHs in tar, as discussed by Godsy *et al.*<sup>21</sup> Compounds which may be lost  
327 from the sediments due to gas ebullition could include mono-, di- and trichlorobiphenyl congeners,  
328 toxaphene and other semi-volatile environmentally persistent organic compounds. Tar migration to  
329 surface water was mostly observed in those areas where both ebullition and tarry sediment were  
330 observed. Whereas, ebullition occurred only in a portion of the tar deposit in which the water was  
331 relatively shallow and sufficient organic matter in the sediment. It is well known fact that ebullition  
332 is a dynamic equilibrium among the degradation of organic carbon, water depth, and sediment  
333 strength, such that no one parameter will control gas bubble generation.<sup>13</sup> It could be concluded from  
334 the results that gas ebullition increased with Darcy flux and the temperature. The possible reason  
335 could be the microbial growth increased with temperature increasing.<sup>10</sup> Microbial activity also  
336 increased the amount of gas levels leading to formation of new gas in deep sediments.<sup>10</sup> So gas

337 production was higher in current study due to the increase in Darcy flux, temperature and microbial  
338 growth in contaminated river sediments, which is inconsistent with previous results.<sup>12, 22</sup> The final  
339 phase of bubble or contaminant transport from sediments was bubble ejection from the sediments,  
340 movement through the water column, and released to the atmosphere. Based on the studies, it was  
341 apparent that the transport of sediment-associated organic compounds by way of sediment bubbles  
342 may be an important pathway. It should be considered in toxic chemical management plans and  
343 models for the Great lakes basin. It was a mechanism by which in place sediment pollutants may be  
344 recycled within the basin and could also represent a pathway whereby contaminants could be  
345 transported outside of the basin.

#### 346 **4. Conclusion**

347 There is no paper reported that the difference between air-water interface and sediment-water  
348 interface gas collection. Hydraulic head gradients and temperature data can be used to estimate  
349 volumes of gas bubbles in sediment. Results showed that a comparatively simple linear relationship  
350 existed between gas flux and measured parameters ( $G_F = 0.316 T + 300.66i$ ,  $R^2 = 0.82$ ). Methods  
351 used in this paper are noninvasive and nondestructive. In addition to providing an in-situ measure of  
352 gas volume, methods presented here provide continuous data, allowing the response of gas volume at  
353 different site to be related to climatic drivers. In addition, these results had implications for capping  
354 design in ebullition-active sediment sites, which proved in situ sand cap could be an effective  
355 remediation for tar contaminated. The analysis presented here has shown that gas flues and reactive  
356 transport modeling can provide effective means of investigating ebullition and quantifying gas  
357 transport. Further work along this modeling using different sites and gas production rates will lead to  
358 a better understanding of the controls on toxic chemical by way of sediment bubbles.

#### 359 **Acknowledgement**

360 Funding for this study was supported by Weston Inc., and Purdue University, the Priority Academic  
361 Program Development of Jiangsu Higher Education Institutions (PAPD), and the Natural Science  
362 Foundation of Jiangsu Province, P.R. China (BK20131287).

363

364 **References**

- 365 1. S. Hyun, C. T. Jafvert, B. Jenkinson, C. Enfield and B. Johnson, *Chemosphere*, 2007, **68**,  
366 1020-1029.
- 367 2. C. T. Jafvert, D. Lane, L. S. Lee and P. S. C. Rao, *Chemosphere*, 2006, **62**, 315-321.
- 368 3. M. D. Mattson and G. E. Likens, 1990.
- 369 4. J. P. Chanton, C. S. Martens and C. A. Kelley, *Limnol. Oceanogr*, 1989, **34**, 807-819.
- 370 5. E. L. McLinn and T. R. Stolzenburg, *Environmental Toxicology and Chemistry*, 2009, **28**,  
371 2298-2306.
- 372 6. D. A. Matthews, S. W. Effler and C. M. Matthews, *Archiv fur Hydrobiologie*, 2005, **163**,  
373 435-462.
- 374 7. J. Zeikus and M. Winfrey, *Applied and environmental microbiology*, 1976, **31**, 99-107.
- 375 8. M. Palermo, T. Thompson and F. Swed, *Response to a document by the Johnson Company:*  
376 *Ecosystem-based rehabilitation plan—An integrated plan for habitat enhancement and*  
377 *expedited exposure reduction in the lower Fox River and Green Bay*, 2002.
- 378 9. N. J. Fendinger, D. D. Adams and D. E. Glotfelty, *Science of the total environment*, 1992, **112**,  
379 189-201.
- 380 10. J. Joyce and P. W. Jewell, *Environmental & Engineering Geoscience*, 2003, **9**, 167-178.
- 381 11. C. S. Martens and J. Val Klump, *Geochimica et Cosmochimica Acta*, 1980, **44**, 471-490.
- 382 12. T. DelSontro, D. F. McGinnis, S. Sobek, I. Ostrovsky and B. Wehrli, *Environmental Science &*  
383 *Technology*, 2010, **44**, 2419-2425.
- 384 13. D. O. Rosenberry, P. H. Glaser, D. I. Siegel and E. P. Weeks, *Water Resources Research*, 2003,  
385 **39**.
- 386 14. D. Reible, D. Lampert, D. Constant, R. D. Mutch Jr and Y. Zhu, *Remediation Journal*, 2006, **17**,  
387 39-53.
- 388 15. P. H. Jacobs, *Water research*, 2002, **36**, 3121-3129.
- 389 16. K. Yin, P. Viana, X. Zhao and K. Rockne, *Science of the Total Environment*, 2010, **408**,  
390 3454-3463.
- 391 17. H. H. Huls and M. Costello, Third International Conference on Remediation of Contaminated  
392 Sediments, New Orleans, LA, 2005.
- 393 18. R. Jepsen, J. McNeil and W. Lick, *Journal of Great Lakes Research*, 2000, **26**, 209-219.
- 394 19. P. Z. Viana, K. Yin and K. J. Rockne, *Environmental science & technology*, 2012, **46**,  
395 12046-12054.
- 396 20. C. W. Beckwith and A. J. Baird, *Water Resources Research*, 2001, **37**, 551-558.
- 397 21. E. M. Godsy, D. F. Goerlitz and D. Grbic - Galic, *Ground Water*, 1992, **30**, 232-242.
- 398 22. R. T. Amos and K. U. Mayer, *Environmental science & technology*, 2006, **40**, 5361-5367.

399

400

401

402 **Figure captions**

403 **Fig. 1** Locations of gas sampling activities. RC6 (top) is near the Hohman Avenue Bridge and the  
404 railroad bridge is evident by the change in surface topography over the river.

405 **Fig. 2** Schematic of sand cap test cell and photograph of gas collection tent at RC3, with gas evident  
406 under the PVC film.

407 **Fig. 3** Schematic of field implementation of the seepage meter system.

408 **Fig. 4** Possible pathway for sediment contaminant transport by gas bubble ebullition.

409 **Fig. 5** Quantity of gas released at different locations, CH<sub>4</sub>, N<sub>2</sub>, and CO<sub>2</sub> comprised  $54.44 \pm 8.22$  %,   
410  $39.72 \pm 8.92$ %, and  $5.83 \pm 1.21$  % (values are means  $\pm$  SD) of the gas by volume, respectively.

411 **Fig. 6** Gas flux in sediment and sand cap. Plot of gas flux versus temperature.

412 **Fig. 7** Comparative graph of the percent of time under discharge conditions with the percent of time  
413 under recharge conditions for the seven river clusters with data loggers.

414 **Fig. 8** Fluctuation of gas flux according to the changes in river elevation and gradient.

415 **Fig. 9** Comparison of measured versus model predicted gas flux. The upper Fig (a) compares  
416 measured gas flux values to regression predicted gas flux (dashed line represents 1:1 slope). The  
417 lower Fig (b) compared Methane flux values versus the vertical hydraulic gradient (Discharge)  
418 values.

419



Figures:

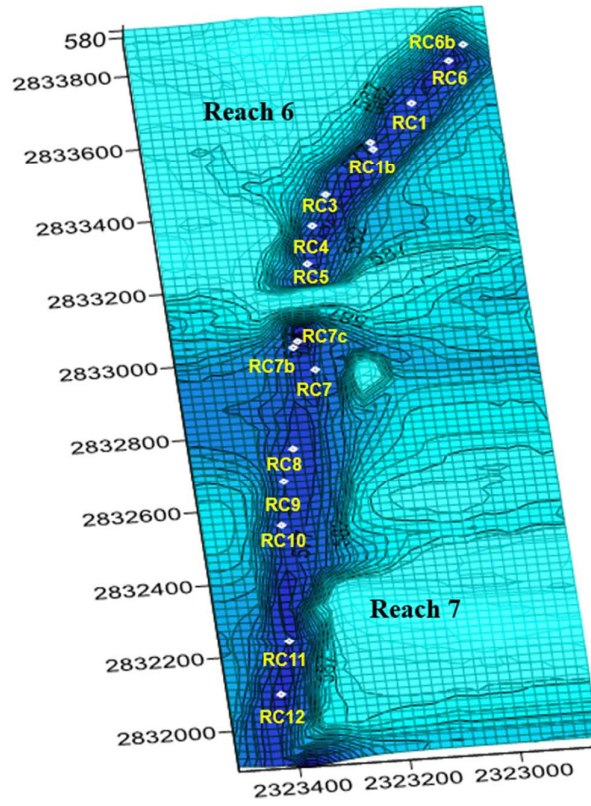


Fig. 1

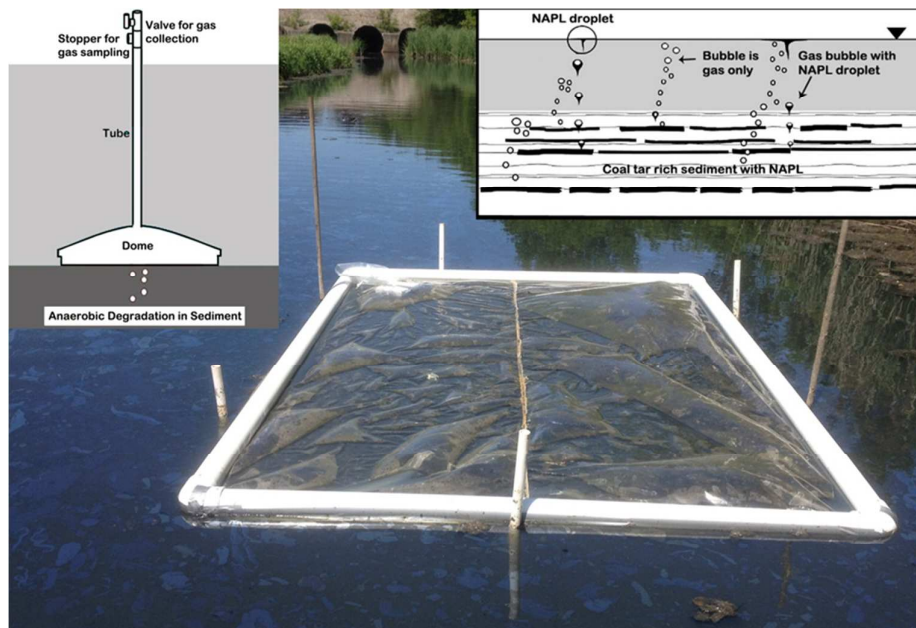


Fig. 2

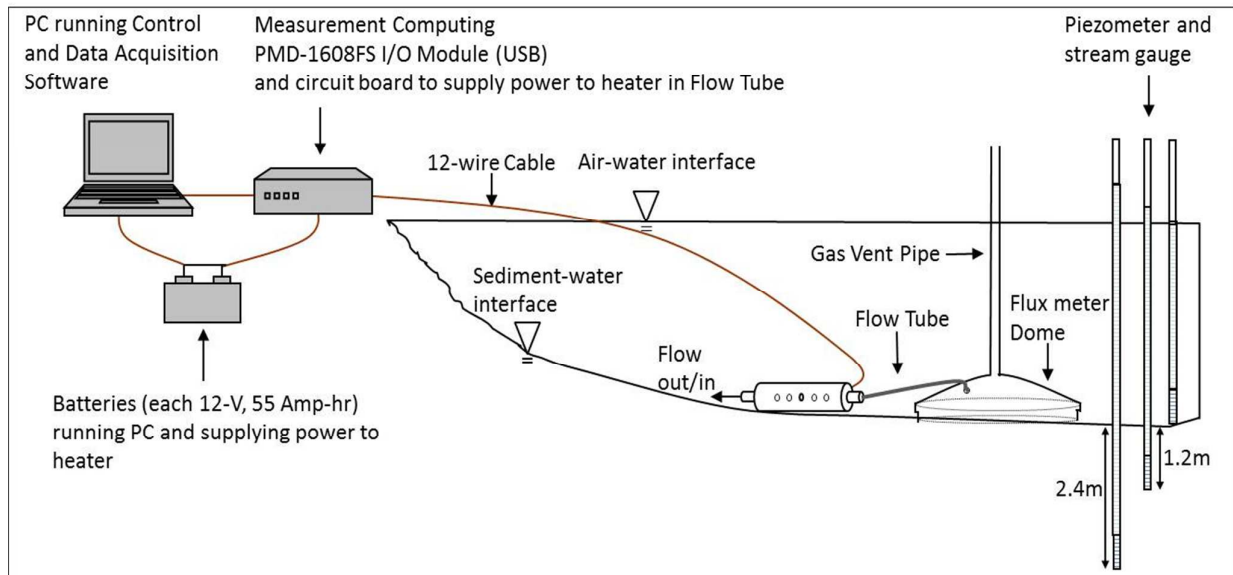


Fig. 3

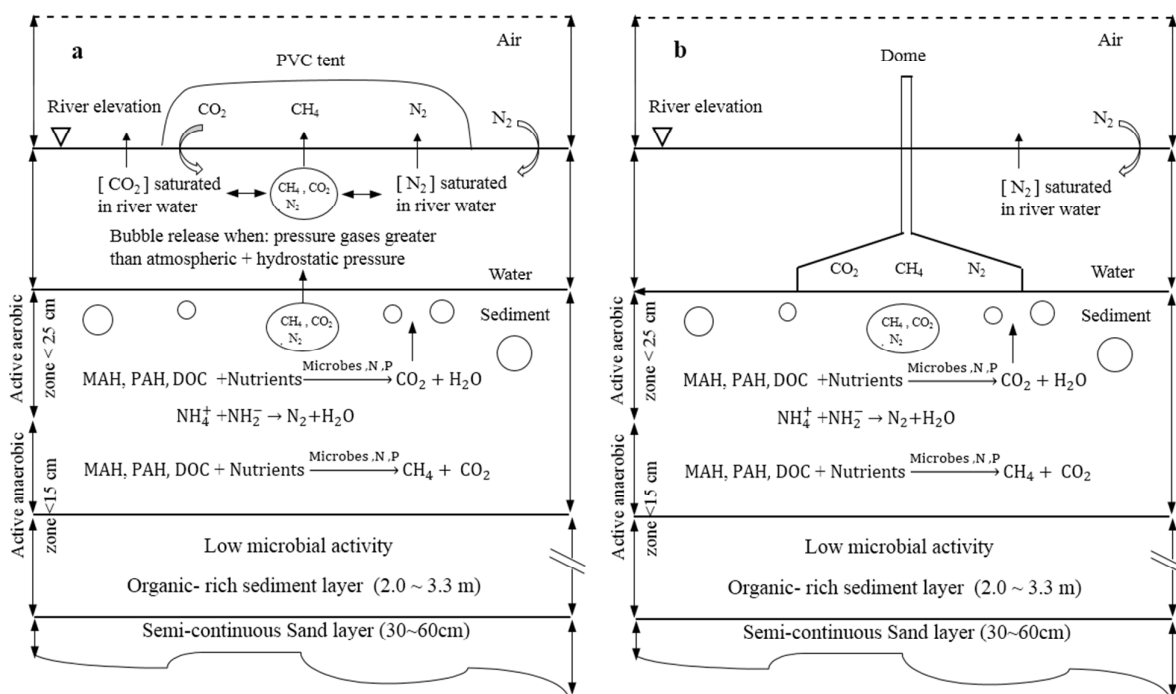


Fig. 4

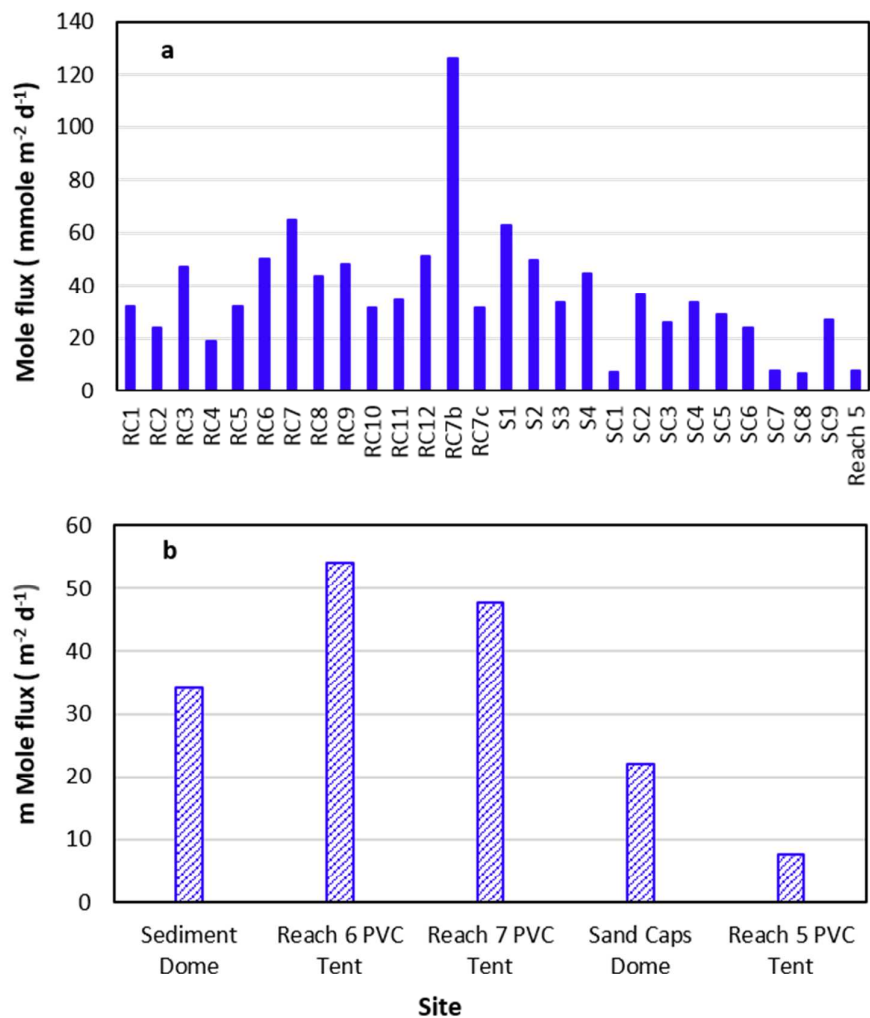


Fig. 5

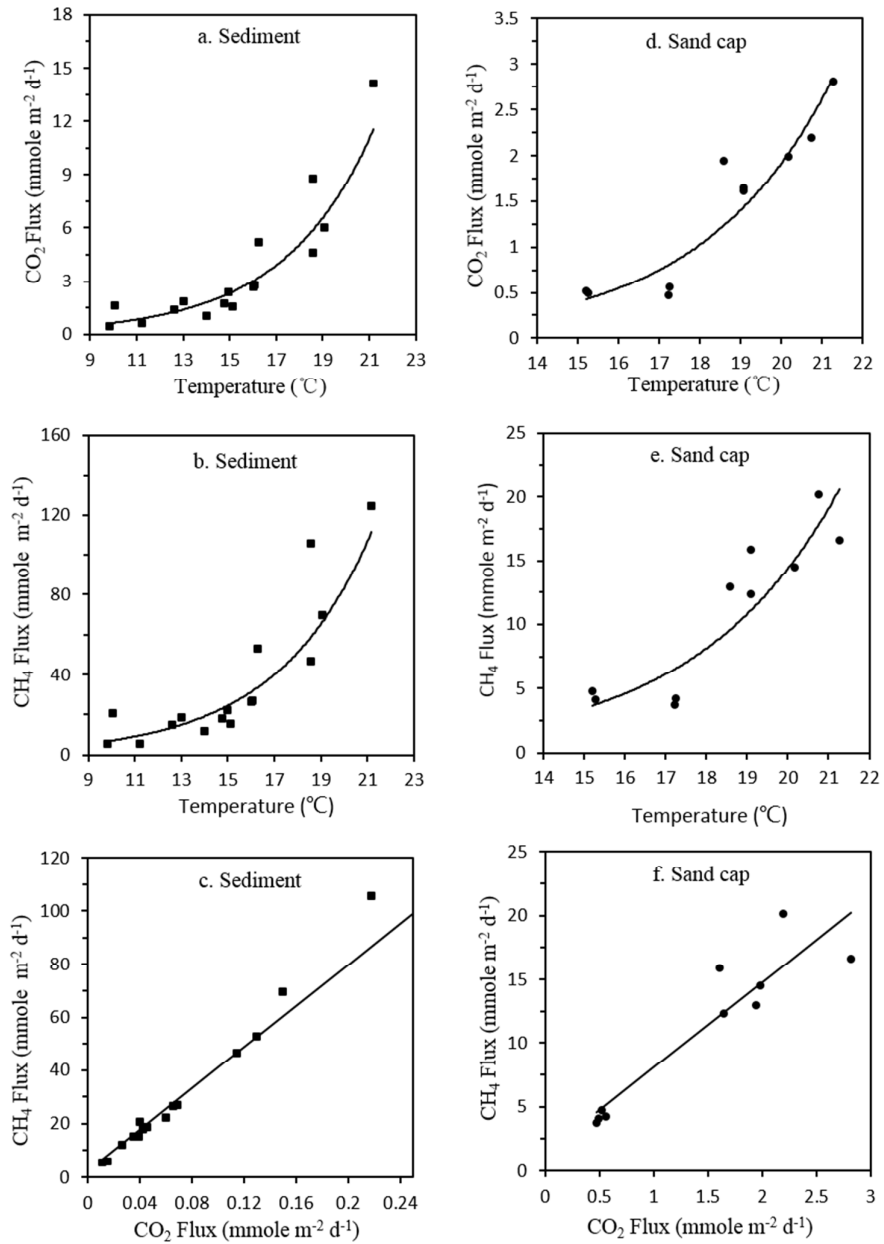


Fig. 6

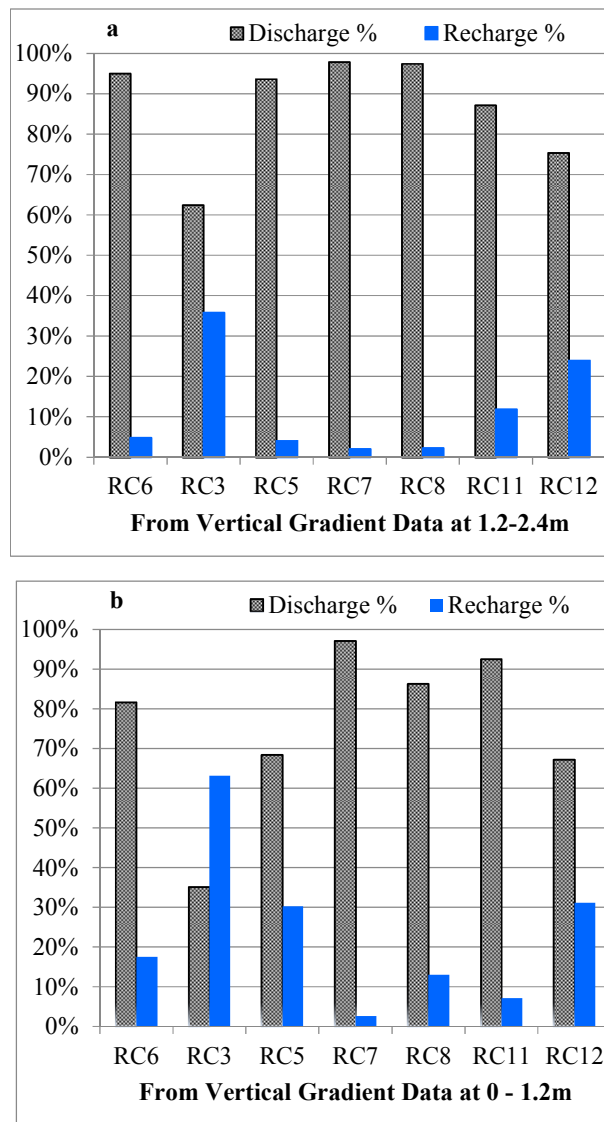


Fig. 7

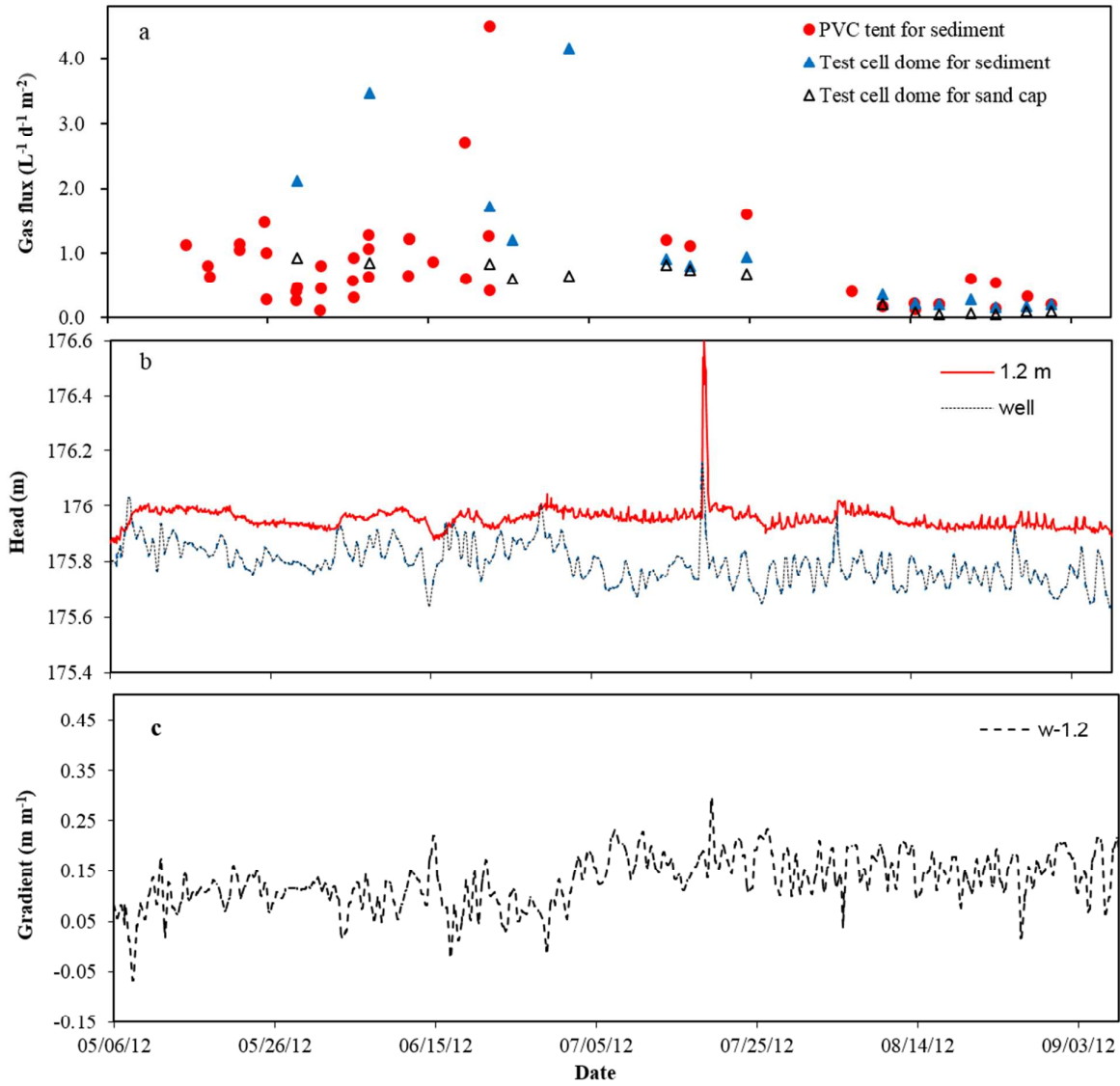


Fig. 8

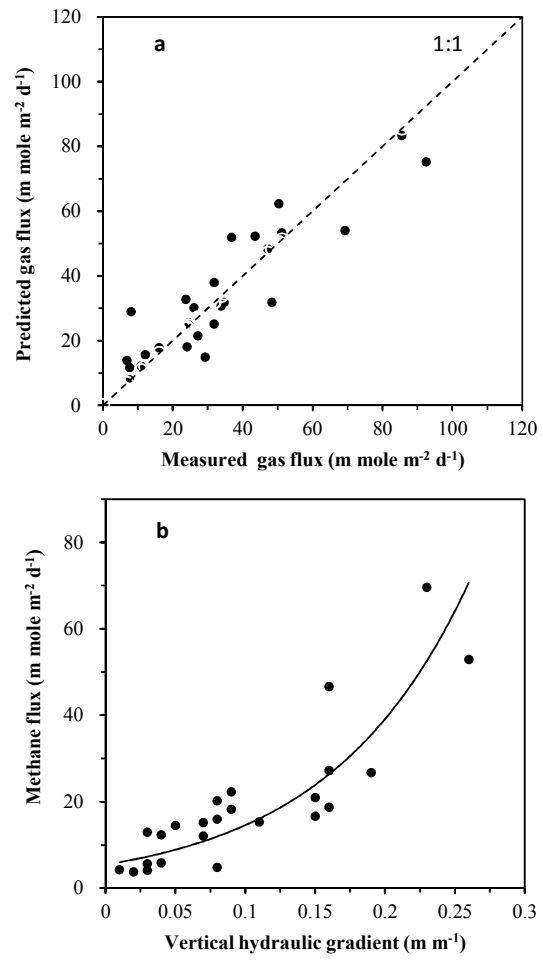


Fig. 9